Meat Science xxx (xxxx) 109073

Contents lists available at ScienceDirect

Meat Science

journal homepage: www.elsevier.com/locate/meatsci

Targeted energy metabolomics analysis of postmortem pork in an *in vitro* model as influenced by protein S-nitrosylation

Wenwei Lu, Qin Hou, Jian Zhang, Wangang Zhang *

Key Laboratory of Meat Processing and Quality Control, Ministry of Education China, Jiangsu Collaborative Innovation Center of Meat Production and Processing, Quality and Safety Control, College of Food Science and Technology, Nanjing Agricultural University, Nanjing 210095, China

ARTICLE INFO

Keywords:
Protein S-nitrosylation
Postmortem energy metabolism
In vitro model
Meat quality
UPLC-MS/MS

ABSTRACT

For exploring the effect of protein S-nitrosylation on the energy metabolism of early postmortem pork (within 24 h postmortem), the six *Longissimus thoracis* (LT) muscle homogenates were treated with nitric oxide donor (NOR-3, (±)-(*E*)-4-Ethyl-2-(E)-hydroxyimino-5-nitro-3-hexenamide), nitric oxide synthase (NOS) inhibitor (L-NAME, Nω-nitro-L-arginine methyl ester hydrochloride) and control (0.1 M K_2HPO_4, pH 7.4) in the *in vitro* buffer system for 24 h, respectively. The western blotting result showed that NOR-3 treatment led to a greater level of protein S-nitrosylation ($p < 0.05$). However, S-nitrosylation levels had no significant difference between L-NAME and control groups ($p > 0.05$). In addition, results showed that 16 significantly differential energy metabolites were identified by ultra-performance liquid chromatography-tandem mass spectrometry (UPLC-MS/MS) and clearly separated among three groups in the principal component analysis. Four pathways (glycolysis, tricarboxylic acid cycle, purine metabolism and pentose phosphate pathway) related to energy metabolism were significantly influenced by different levels of protein S-nitrosylation. Furthermore, the correlation analysis of metabolites demonstrated that metabolites were in dynamic equilibrium with each other. These results indicate that protein S-nitrosylation can participate in and regulate energy metabolism postmortem pork through glycolysis and tricarboxylic acid (TCA) cycle.

1. Introduction

Post-translational modification of protein is a complex process, which modulates structural and functional properties of protein including catalytic activity, protein stability, oligomeric state, binding of allosteric activators and conditional protein interaction (Liu, Warner, Zhou, & Zhang, 2018; Warner, Dunshea, Ponnampalam, & Cottrell, 2005). The modification types include S-nitrosylation, phosphorylation, oxidation, acetylation, methylation, hydroxylation and others. As a typical redox-dependent post-translational modification of the protein, protein S-nitrosylation is formed by covalently combining the sulfhydryl group of protein cysteine with nitric oxide (NO) (Stamler & Meissner, 2001). NO-mediated protein S-nitrosylation can exert important influences on the conversion of muscle to meat *via* regulating postmortem crucial pathways, ultimately affecting the quality of meat (Hou, Liu, Tian, & Zhang, 2020; Li et al., 2014; Liu et al., 2018; Warner et al., 2005; Zhang, Marwan, Samaraweera, Lee, & Ahn, 2013).

The energy metabolism of postmortem muscle plays an important role in determining the quality of fresh meat during the conversion of muscle to meat. However, the abnormal energy metabolism of postmortem muscle can affect the extent and rate of pH changes, which in turn adversely influence the tenderness, color and water holding capacity of meat (Bee, Anderson, Lonergan, & Huff-Lonergan, 2007; Wang et al., 2019). Interestingly, Liu et al. (2019) found that many enzymes involved in postmortem energy metabolism could be modified by protein S-nitrosylation. Our lab also showed that the activities of phosphofructokinase and glyceraldehyde-3-phosphate dehydrogenase were inhibited by protein S-nitrosylation in postmortem pork (Zhang et al., 2019). Between the pale, soft and exudative and red, firm and non-exudative pork, Wang et al. (2020) indicated that there were significant differences in S-nitrosylation levels and enzyme activities of phosphofructokinase, pyruvate kinase and glycogen phosphorylase. These results indicate that protein S-nitrosylation may affect meat quality by regulating postmortem energy metabolism. Thus, it is of great significance to ex-

* Corresponding author at: National Center of Meat Quality and Safety Control, College of Food Science and Technology, Nanjing Agricultural University, Nanjing, Jiangsu 210095, China.
E-mail address: wangang.zhang@njau.edu.cn (W. Zhang).

https://doi.org/10.1016/j.meatsci.2022.109073
Received 16 December 2021; Received in revised form 14 November 2022; Accepted 7 December 2022
0309-1740/© 20XX

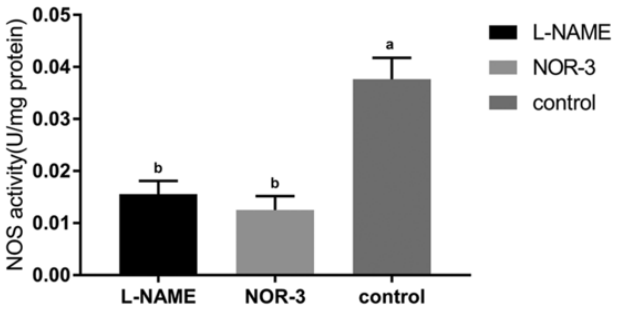

Fig. 1. NOS activity in the *in vitro* reactions at 24 h. All measurements were expressed as the mean ± SE. a–b: Different letters are significantly different between treatments ($p < 0.05$, $n = 6$).

plore how the protein S-nitrosylation influences energy metabolism for further regulating the quality of fresh meat.

Several methods have been applied to analyze energy metabolism in postmortem muscle including one-dimensional proton nuclear magnetic resonance (^{1}H NMR) and UPLC-MS/MS (Cônsolo et al., 2021; Yu, Tian, Shao, Li, & Dai, 2019). Compared with ^{1}H NMR, UPLC-MS/MS has significant advantages of a strong precision and a high detection sensitivity for the quantitative and qualitative identification of energy metabolites. In addition, UPLC-MS/MS has been widely used for the absolute quantification analysis of target metabolites in food analysis. Yu et al. (2019) revealed that energy metabolism between the bovine *psoas major* (PM) and *longissimus lumborum* (LL) during early postmortem periods by UPLC-MS/MS targeted metabolomics. Cônsolo et al. (2021) found that the development of dark-cutting beef was closely related to the energy metabolism pathway. However, the targeted energy metabolomics analysis of postmortem pork as influenced by protein S-nitrosylation has not been reported.

Therefore, the present research was designed to investigate the targeted energy metabolite variation of early postmortem pork in an *in vitro* model as influenced by different levels of protein S-nitrosylation using UPLC-MS/MS based metabolomics multivariate statistical analysis (orthogonal projections to latent structures discriminant analysis, principal components analysis, hierarchical cluster analysis and correlation analysis). Furthermore, significantly different metabolic pathways were also analyzed, aiming to reveal the influential mechanism of protein S-nitrosylation on energy metabolism in postmortem pork.

2. Materials and methods

2.1. Sample preparation

According to the national standard slaughter procedure (GB/T 19479–2019), six castrated crossbred (Duroc × Landrace × Yorkshire) pigs aged 6 months (100 ± 10 kg) were harvested in a local slaughterhouse (Sushi Company, Huai'an, China). All pigs were reared in a large-scale intensive rearing mode with same feeding environment. Pigs were humanely harvested by electrical stunning and *Longissimus thoracis* (LT) were removed from the left side of the carcass at 0.5 h postmortem (average weight of 500 ± 5 g). After sampling, a portion of the meat sample (approximately 200 g) was stored at 4 °C for pH and color measurement. Meanwhile, the remaining portion of meat was immediately frozen with liquid nitrogen and stored at −80 °C for further analysis. On the basis of the criteria proposed by Warner, Kauffman, and Greaser (1997), the pH and color of pork samples were measured at 1 h and 24 h and all parameters were within the normal ranges.

2.2. In vitro buffer system

A total of 0.5 g pork samples ($n = 6$) were ground into powder in liquid nitrogen. The samples were taken out from liquid nitrogen and then homogenized in the phosphate buffer (0.1 M K_2HPO_4, pH 7.4) at a ratio of 1:2 (wt/vol). Then the samples were incubated at 37 °C for 1 h with the following three treatments at the ratio of 1:1 (vol/vol): control (phosphate buffer), 1 mM NOR-3 (NO donor, (±)-(*E*)-4-Ethyl-2-(E)-hydroxyimino-5-nitro-3-hexenamide, E2895, Sigma-Aldrich Corp) and 0.1 M L-NAME (NOS inhibitor, Nω-nitro-L-arginine methyl ester hydrochloride, N5751, Sigma-Aldrich Corp), respectively. Following this, the reaction buffers were added to the mixtures at a ratio of 1:5 (mixtures vol/reaction buffers vol) for building *in vitro* model and incubated at 25 °C (Matarneh, Beline, Silva, Shi, & Gerrard, 2018). After completing the incubation for 24 h, samples (10 mL) were taken out with a pipette after mixing well from the reaction buffer for the following analysis. The reaction buffers contained 10 mM Na_2HPO_4, 0.5 mM nicotinamide adenine dinucleotide (NAD (+)), 60 mM KCl, 30 mM creatine, 5 mM adenosine 5′-triphosphate (ATP), 40 mM glycogen, 0.5 mM adenosine 5′-diphosphate, 5 mM $MgCl_2$, 10 mM sodium acetate and 25 mM carnosine.

2.3. NOS activity

The sample (1 mL) was centrifuged at 4 °C and 10,000 g for 14 min, and then the activity of NOS in the supernatant was measured using NOS activity assay kit (A014–2-2, Nanjing Jiancheng Bioengineering Institute, China). Protein concentration was determined using the bicinchoninic acid protein assay kit (PC0020, Beijing Solarbio Science & Technology Co., Ltd., China).

2.4. Protein S-nitrosylation level

Referring to the method of Wang et al. (2019), the level of protein S-nitrosylation was measured using the pierce S-nitrosylation western blot kit (90,105, Thermo Fisher Scientific, USA). Firstly, the samples (1 mL) were centrifuged at 4 °C and 10,000 g for 15 min. The supernatant was removed from the pellet and then 1 M methyl methanethiosulfonate (20 μL) was added into the supernatant. Then the mixtures were incubated at 25 °C for 0.5 h to block free cysteine thiols. Next, the sample (1 mL) was added with 6 mL pre-chilled acetone and then frozen at −20 °C for 1 h to remove methyl methanethiosulfonate. The samples and tubes were inverted to decant the acetone after centrifuge and then pellet was redissolved with HENS buffer (200 μL; 1 mM ethylene diamine tetraacetic acid, 0.1 M 2-[4- (2-hydroxyethyl) piperazin-1-yl] ethanesulfonic acid, 1% sodium dodecyl sulfate, 0.1 mM neocuproine, pH 7.8). To irreversibly bind with the cysteine thiol, the dissolved iodo tandem mass tags reagent (20 μL) and 1 M sodium ascorbate (40 μL) were added to the 200 μL samples. Finally, the reaction solutions were incubated at 37 °C for 1 h under dark conditions.

The labeled protein was analyzed by sodium dodecyl sulfate-polyacrylamide gel electrophoresis (SDS-PAGE) and western blotting. Proteins were dissolved in SDS-PAGE loading buffer (P1040, Beijing Solarbio Science & Technology Co., Ltd., China). The loading buffer (pH 6.8) consisted of 50% glycerol, 60 mM Tris-HCl, 2% SDS, 1% DTT and 0.1% bromophenol blue. Proteins were separated by SDS-PAGE on 10% gels and transferred to polyvinylidene difluoride membranes (ISEQ00010, Millipore, Germany) with a pore size of 0.2 μm. Following this, the membranes were blocked with 5% non-fat milk at room temperature for 1 h (RP0004, Ryon Biological Technology, China). The anti-tandem mass tag antibody (mouse monoclonal antibody; 1:1000; 90,105, Thermo Fisher Scientific, USA) was used to treat the membranes for 14 h as a primary antibody. Then the mouse anti-rabbit immunoglobulin antibody (1:5000; A01827, GenScript, China) was used to treat the membranes for 1 h as the second antibody. Finally, the membranes were reacted with the peroxide solution and ECL substrate (34,580, Thermo Fisher Scientific, USA). The relative amounts of proteins were semi-quantified by Image Quant LAS4000 (GE, CT, USA).

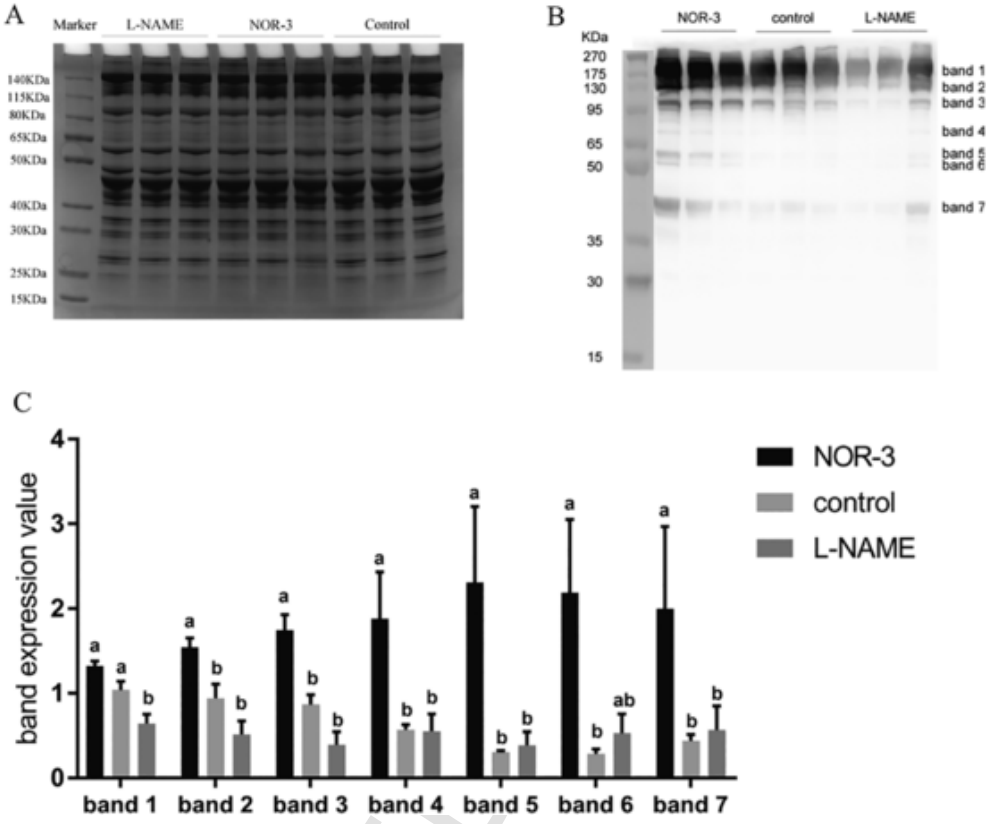

Fig. 2. The S-nitrosylation levels of total protein in the *in vitro* reactions at 24 h. (A) Representative image of SDS-PAGE of the samples before the procedure of iodoTMT method. (B) Western blot analysis of S-nitrosylated protein after iodoTMT labeling. (C) Band abundance value of S-nitrosylated protein. All measurements were expressed as the mean ± SE. a–b: Different letters are significantly different between treatments ($p < 0.05$, n = 6).

The protein S-nitrosylation level was calculated depending on the ratio of enriched S-nitrosylation protein and total protein.

2.5. Targeted metabolomics analysis

A total of 38 key metabolites involved in the pentose phosphate pathway (PPP), glycolysis pathway, oxidative phosphorylation and tricarboxylic acid cycle (TCA cycle) were detected simultaneously by UPLC-MS/MS.

2.5.1. Metabolites extraction

Each sample (100 μL) was taken out from the reaction buffer following by extracting with precooled water (100 μL) and methanol/acetonitrile (800 μL, 1:1, vol/vol). Then the samples were mixed and treated with ultrasound (20 kHz frequency, 100 W) for 60 min in the ice bath. The samples were centrifuged at 15,000 *g* and 4 °C for 25 min. Following this, the succinate D6 and glutamate D5 were added to each sample and then the samples were vacuum dried. For mass spectrometry, the samples were redissolved and then acetonitrile and water solutions (100 μL, 1:1, vol/vol) were added. Finally, 80 μL supernatants were taken out from the mixtures for further analysis.

2.5.2. UPLC-MS/MS measurement

The measurement was performed by Shimadzu Nexera X2 LC-30AD UPLC. Mobile phase: solution A was consisted of 5% acetonitrile and 10 mM ammonium acetate (pH 9.0); and solution B was consisted of 95% acetonitrile and 10 mM ammonium acetate (pH 9.0). The sample was redissolved in 50% acetonitrile (100 μL) in the autosampler at 4 °C. The injection volume was 5 μL. The column (ACQUITY UPLC BEH Amide 1.7 μm, 2.1 mm × 100 mm column; Waters, Ireland) temperature was 40 °C. The flow rate was 300 μL/min. The gradient of related mobile phase was as follows: in 0–2 min, solution B was maintained at 95%; 2–9 min, solution B was linearly changed from 95% to 70%; 9–10 min, solution B was linearly changed from 70% to 30%; 10–11 min, solution B was maintained at 30%; 11–11.5 min, solution B was linearly changed from 30% to 95%; and 11.5 to 15 min, solution B was maintained at 95%.

Mass spectrometry was performed using a QTRAP5500 mass spectrometer (AB SCIEX) in positive and negative ion mode. The experiment parameters were set as follows: curtain gas, 35 psi; ion source gas 1, 40 psi; ion source gas 2, 50 psi; and source temperature, 550 °C. The experiment parameters of ion spray voltage floating for positive and negative ion mode were set as 5500 V and 4500 V, respectively.

2.6. Statistical analysis

The original MS/MS data were retrieved by software MS-Dial (Version 4.16) and matched with a standard database, HMDB and MassBank public databases. The remaining missing values were filled with 1/2 minimum value. Then the total peak area was normalized and the retention time was extracted by MultiQuant software. The calibration retention time of standard samples was used for metabolite identification. The peak area of metabolite extracted ions was normalized by internal criteria succinate D6 and glutamate D5.

Data were presented as mean ± standard error (SE). Statistical analysis system (SAS Institute Inc., Cary, NC) was employed to perform one-way analysis of variance (ANOVA). The Duncan's multiple range tests were used to compare differences in the individual groups ($p < 0.05$). All figures were performed with the SigmaPlot 13.0 software on Windows.

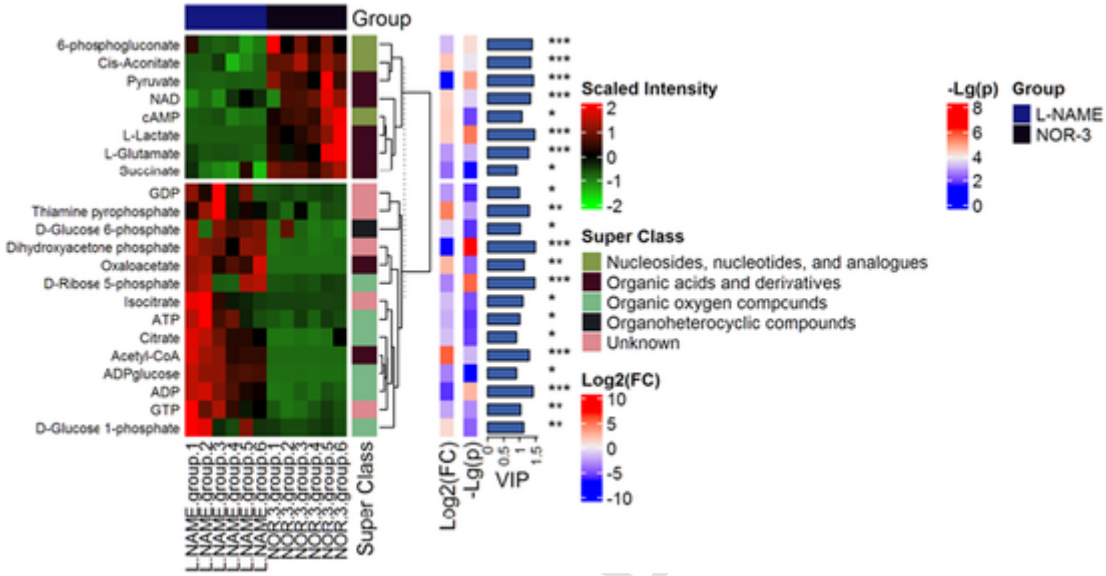

Fig. 3. Complex heatmap of metabolites in the different treatments (L-NAME and NOR-3).

3. Results and discussion

3.1. NOS activity

The NOS activity of different groups is shown in Fig. 1. The result showed that no significant difference in NOS activity was observed between NOR-3 and L-NAME groups ($p > 0.05$). However, compared with the control group, the NOS activity was significantly decreased after NOR-3 and L-NAME treatments ($p < 0.05$). NOS activity can reflect the potential capacity of NO production in skeletal muscle. L-NAME could inhibit the NOS activity due to the competitive relationship between L-NAME and L-arginine which is the substrate for NO production. Lower NOS activity in NOR-3 group might be due to the excessive NO content in muscle cells, which could have a feedback inhibition effect on NOS as shown in our previous study (Zhang et al., 2019). Previous work has demonstrated that NOS activity in fresh chicken thigh muscle was not affected over the pH range of 4.5–7.4 (Brannan & Decker, 2002). Therefore, the effects of NOR-3 and L-NAME treatment on NOS activity were much greater than pH and substrate exhaustion. Similarly, our previous work has demonstrated that the red, firm and non-exudative pork had higher NOS activity than that of pale, soft and exudative samples (Wang et al., 2019). Thus, the change of NOS activity may lead to the different levels of NO production and then affect postmortem biochemical reactions and meat quality.

3.2. Protein S-nitrosylation level

As shown in Fig. 2 **(A)**, SDS-PAGE showed similar number and strength of major protein bands in three groups before iodo tandem mass tags labeling for determining protein S-nitrosylation level ($p > 0.05$). As shown in Fig. 2 **(B)**, western blotting analysis showed that S-nitrosylation levels had no significant difference between L-NAME and control groups ($p > 0.05$). This phenomenon could be attributed to the fact that S-nitrosylated protein was difficult to be detected if the amount of S-nitrosylated protein was too low. However, NOR-3 group had a significantly higher protein S-nitrosylation level compared to L-NAME group ($p < 0.05$). The distributions of protein S-nitrosylation in the range of 30–100 kDa and 250 kDa were more concentrated and the high abundance suggests that small molecule proteins are more susceptible to S-nitrosylation.

According to the previous study, Liu et al. (2019) found the molecular weight of S-nitrosylated proteins was concentrated within 100 kDa and glycogen metabolism was one of the most significant metabolic pathways for S-nitrosylation proteins. Besides, Zhu, Xing, Hou, Liu, and Zhang (2021) also reported that the S-nitrosylation levels of energy metabolism enzymes were up-regulated in high ultimate pH beef compared to intermediate ultimate pH. These findings suggest that most energy metabolism enzymes may be S-nitrosylated.

3.3. Identification of targeted energy metabolites

The extracted ion chromatogram diagram of energy metabolite standard is shown in **Fig. S1**. The figure shows that the chromatographic peak of each metabolite was well separated. The peak shape was sharp and symmetrical indicating it could be used for mass spectrometry quantization of each metabolite. All samples were equally mixed as quality control samples, which were used to assess the repeatability and stability of the data. The relative standard deviation (RSD) results of the substances are shown in **Fig. S2**. The result of energy metabolites with RSD was <30%, which indicates that the data are stable and reliable.

The concentration of each metabolite is shown in **Table S2**. The results showed that 38 energy metabolites were identified by UPLC-MS/MS with targeted metabolic profiling. Yu et al. (2019) found that 22 metabolites were identified by UPLC-MS/MS in bovine PM and LL muscles during the first 24 h postmortem. Based on ^{1}H NMR, Cônsolo et al. (2021) found 45 metabolites were quantified in the dark-cutting beef samples. In present study, these 38 metabolites were classified into five pathways including glycolysis, oxidative phosphorylation, PPP, TCA cycle and purine metabolism. As shown in **Table S2**, metabolites were dominant in glycolysis metabolism, TCA cycle and PPP, which is consistent with the study of energy metabolites in bovine PM and LL muscles (Yu et al., 2019).

3.4. Changes of metabolite in the in vitro model

3.4.1. Glycolytic metabolites

For glycolytic pathway, the contents of pyruvate, lactate, glucose-1-phosphate (G1P) and glucose-6-phosphate (G6P) were quantified (Fig. 3). Pyruvate and lactate, as important metabolites in glycolysis, were significantly overabundant in NOR-3 group compared with L-NAME and control groups ($p < 0.05$). This result demonstrates that protein S-nitrosylation could regulate the rate of glycolysis. Consistent with our finding, Young, Radda, and Leighton (1997) also found that sodium nitroprusside (NO donor) treatment increased the rate of glucose oxida-

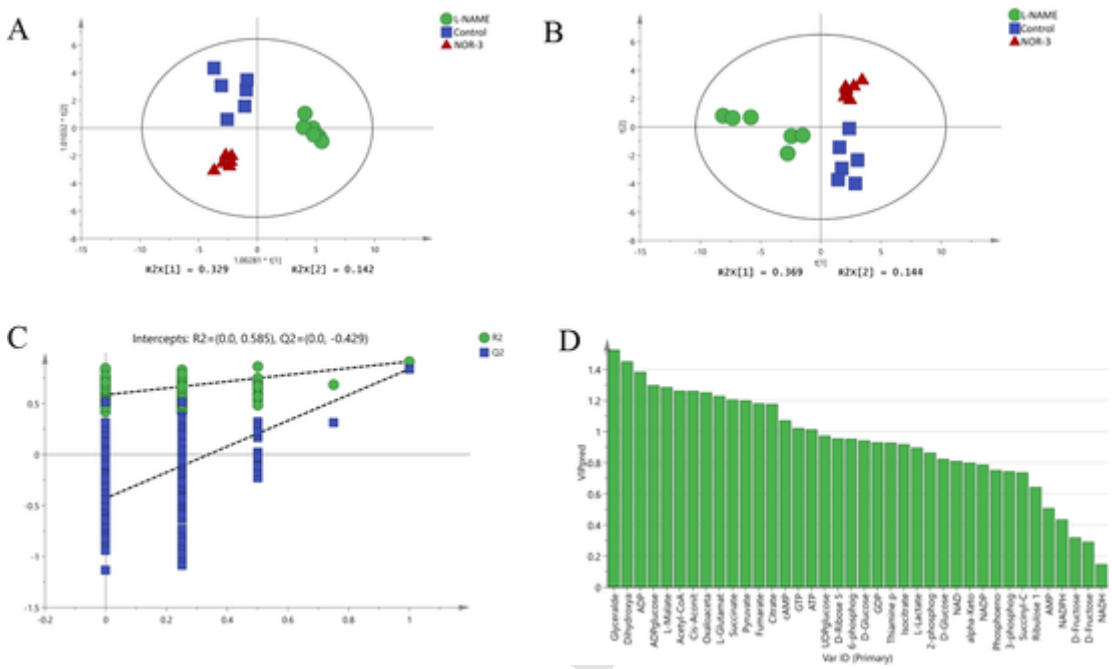

Fig. 4. Comparative analysis of metabolites among different treatments (control, L-NAME and NOR-3). (A): PCA score plot; (B): OPLS-DA score plot; (C): permutation plot, R^2 (cumulative interpretation ability of the model) and Q^2 (predictive ability of the model); (D): VIP $_{(pred)}$ (variable importance for predictive components) plot.

tion, pyruvate and lactate accumulation in rat soleus muscle and the effect was independent of insulin. In addition, NOR-3 group had significantly lower concentration of G6P and G1P compared with L-NAME group ($p < 0.05$). This phenomenon could be attributed to the fact that intermediate metabolites in NOR-3 group were utilized faster than L-NAME group (Matarneh, Yen, Bodmer, El-Kadi, & Gerrard, 2021). Interestingly, Carafoli (2002) indicated that a high level of calcium concentration in sarcoplasm could increase the rate of energy metabolism and lactate formation. In addition, Wang et al. (2019) demonstrated that higher S-nitrosylation levels of sarcoendoplasmic reticulum Ca^{2+}-ATPase (muscle type) and ryanodine receptor channel (muscle type) could induce calcium imbalance in muscle, which in turn accelerated pH decline. Therefore, the changes of glycolysis rate could be related to the different calcium concentrations in the cytoplasm induced by the protein S-nitrosylation.

3.4.2. TCA cycle metabolites

For TCA cycle, the contents of cis-aconitate, succinate, citrate, oxaloacetate, isocitrate, acetyl coenzyme A and glutamate were quantified. As shown in **Table S2** and Fig. 3, the concentration of cis-aconitate and succinate in NOR-3 group was significantly higher than L-NAME group ($p < 0.05$). Previous researches have reported similar results that TCA cycle could continue to produce energy during the first 2 h postmortem and the succinate content changed with time in the *in vitro* model (Matarneh et al., 2021). In addition, Merry, Steinberg, Lynch, and Mcconell (2009) demonstrated that NO might be involved in regulating glucose consumption in muscle cells. Thus, the results demonstrated that more glycogen was consumed in NOR-3 group, leading to the generation of high level of pyruvate, which further increased the contents of cis-aconitate and succinate through the TCA cycle. Furthermore, the contents of citrate, oxaloacetate, isocitrate and acetyl coenzyme A in L-NAME group were significantly increased compared with NOR-3 group ($p < 0.05$). Previous studies have found that glycolysis, pyruvate conversion to lactate, TCA cycle and mitochondrial dysfunction were significant metabolic pathways in postmortem pork involving protein S-nitrosylation (Liu et al., 2019). Similarly, Chouchani et al. (2010) demonstrated that aconitase involved in the TCA cycle was inhibited by S-nitrosylation modification, thus affecting isocitrate metabolism in rat heart mitochondria. S-nitrosylation reactions require negative electrostatic potentials for amino acid residues adjacent to cysteine residues on the protein surface or within the protein. Thus, change of metabolites content may be explained by the fact that different modification sites could exert different effects for enzymes activity (Zhang et al., 2017).

Interestingly, the content of glutamate was significantly higher in NOR-3 group compared to L-NAME group ($p < 0.05$). It might be attributed to the fact that the glutamate could be converted to alpha-ketoglutarate with pyruvate or oxaloacetate under the catalysis of enzymes (Hertz & Chen, 2017). Previous research has shown that S-nitrosylation modification of phosphofructokinase (cysteine 351) reduced the content of TCA cycle metabolites, such as citrate, fumarate, pyruvate, glutamate and alpha-ketoglutarate (Gao et al., 2021). Combined with the present results, we speculated that a protein S-nitrosylation dependent mechanism might affect the energy metabolism of postmortem muscle resulting in the change of pork quality.

3.4.3. Purine and cofactors

For purine and cofactors metabolism, the contents of ATP, cyclic adenosine monophosphate (cAMP) and NAD (+) were quantified (Fig. 3). In present study, L-NAME group had a significantly greater ATP content compared to NOR-3 group ($p < 0.05$). Cônsolo et al. (2021) found that dark-cutting beef showed greater levels of ATP compared to the normal quality samples, which might be related to mitochondrial activity. Furthermore, Escames et al. (2007) found that NO could regulate mitochondrial respiration attributing to the inhibition of NO on cytochrome oxidase. Therefore, the increase of metabolite content in present work was possibly due to the regulation effect of S-nitrosylation on the enzyme activities in mitochondria. The content of cAMP in NOR-3 group was significantly higher than that in L-NAME group ($p < 0.05$). cAMP, as an important second messenger, is generated by the hydrolysis reaction of ATP under the catalysis of adenylate cyclase, which could activate protein kinase A (Moutinho, Hussey, Trewavas, & Malho, 2001). This result could explain the decrease of ATP content in the NOR-3 group. The content of NAD (+) was significantly higher in NOR-

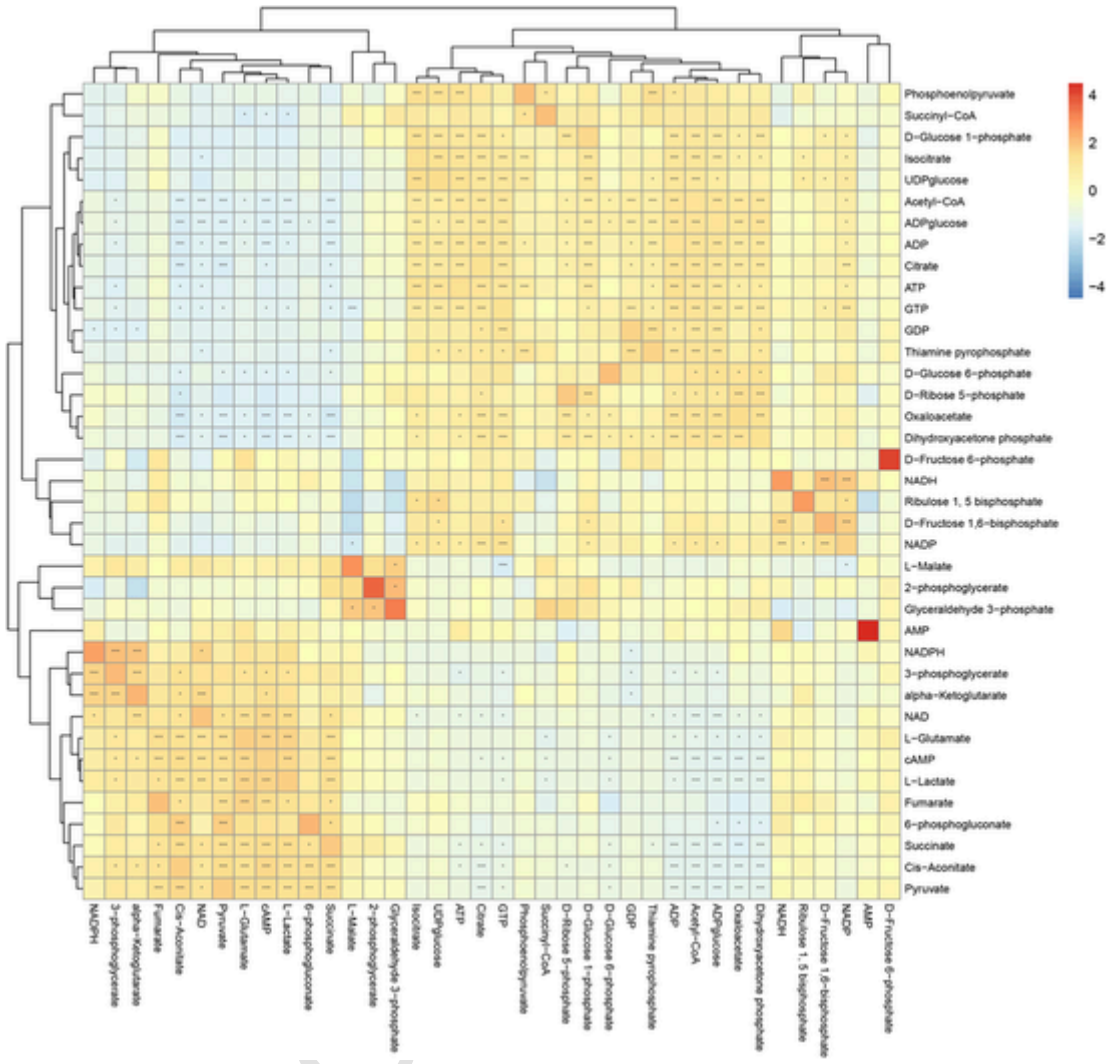

Fig. 5. The correlation map of metabolites in the different treatments (L-NAME and NOR-3). The correlation coefficient (Pearson Correlation value R) between metabolites with significant differences was between −1 and + 1. The correlation coefficient R between metabolites is represented by color, where $R > 0$ indicates positive correlation, which is represented by red. $R < 0$ indicates negative correlation, which is represented by blue. Significant differences of metabolites correlation were displayed as: *, $p < 0.05$; **, $p < 0.01$; ***, $p < 0.001$. (For interpretation of the references to color in this figure legend, the reader is referred to the web version of this article.)

3 group than that of L-NAME group ($p < 0.05$). NAD (+) is the acceptor of the dehydrogenation in the TCA cycle, and it could be transformed by NADH when pyruvate is reduced to lactate (Wells, Selvadurai, & Tein, 2009). These facts could explain the higher lactate content in NOR-3 group compared to L-NAME group. Meanwhile, the overabundance of NAD (+) in NOR-3 group may suggest more intensive pyruvate metabolism than L-NAME group. In addition, the level of NAD (+) has been reported to be significantly higher in LL muscle than other muscle parts (PM or vastus intermedius) because of the higher activities of energy metabolism enzymes in LL (Muroya, Oe, Nakajima, Ojima, & Chikuni, 2014; Yu et al., 2019).

3.4.4. Pentose phosphate pathway

The PPP is one of the most important pathways in glucose catabolism. In present study, the content of 6-phosphogluconate in NOR-3 group was significantly higher than L-NAME group while L-NAME group showed significantly greater ribose 5-phosphate content compared to NOR-3 group ($p < 0.05$). Aliani, Farmer, Kennedy, Moss, and Gordon (2013) found that the content of ribose 5-phosphate in most chickens reached its peak at 28–55 h after slaughter and gradually decreased after refrigeration. This phenomenon might be due to the formation of ribose 5-phosphate by oxidative decarboxylation and molecular rearrangement of 6-phosphogluconate. Previous studies have shown that the rate of energy metabolism was controlled by regulating the balance of G6P consumption in the pentose phosphate and the glycolysis pathways when treating astrocytes with NO (Bolaños, Delgado-Esteban, Herrero-Mendez, Fernandez-Fernandez, & Almeida, 2008).

3.5. Multivariate statistical analyses of metabolites

3.5.1. Principal components analysis (PCA)

In the PCA plot (Fig. 4 **(A)**), the first principal component (PC1) and the second principal component (PC2) accounted for 36.9% and 14.4%, respectively. The control group was noticeably separated from the L-NAME and NOR-3 groups along with PC1. Furthermore, L-NAME group was obviously separated from NOR-3 group along with PC2. Similarly, Yu et al. (2019) revealed that PM was obviously separated from LL muscle samples in the PCA results possibly due to the different activities of energy metabolism enzymes. The present result indicates that the metabolite patterns were clearly changed after regulating the level of protein S-nitrosylation, which is in concert with the absolute quantita-

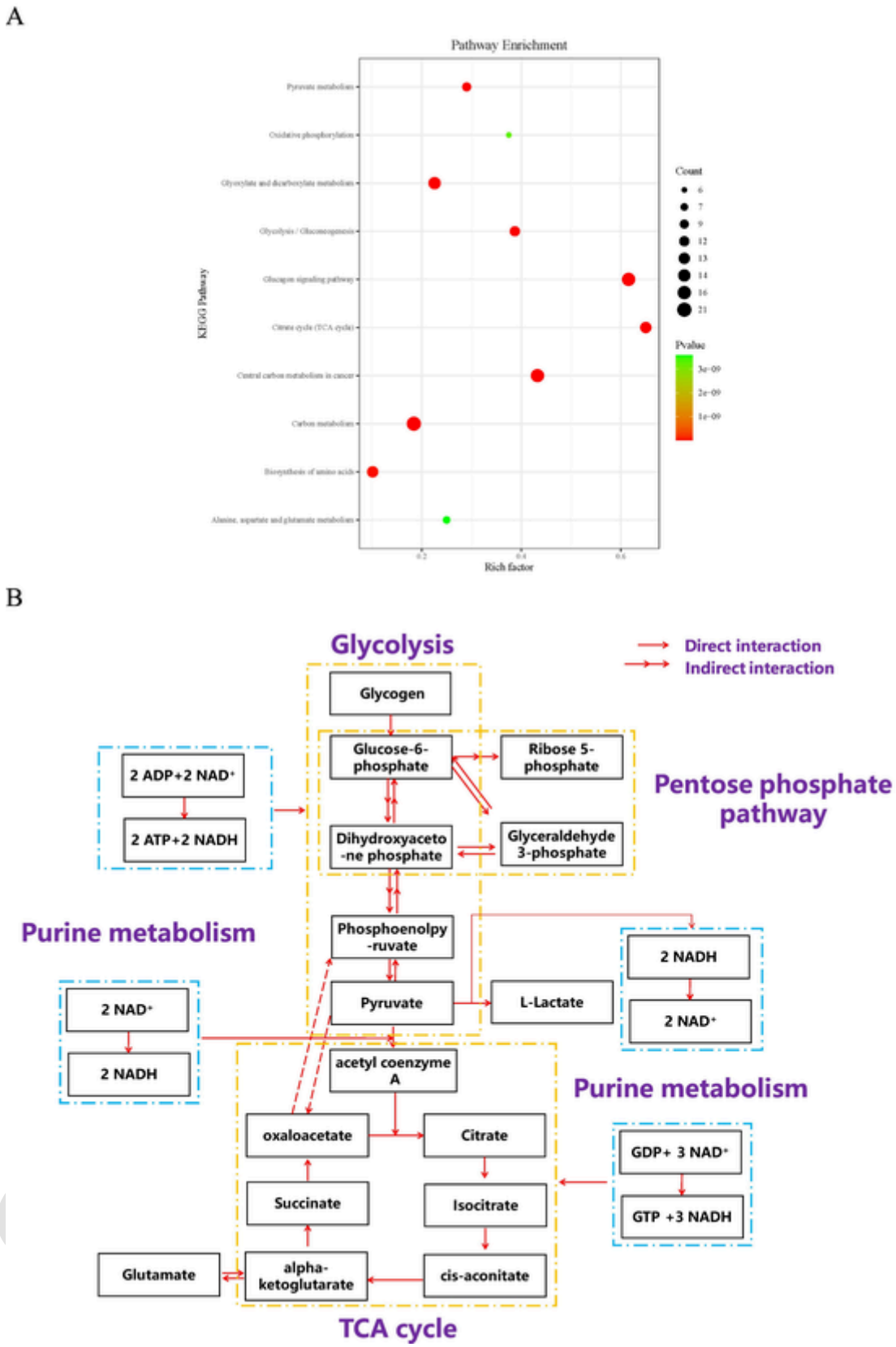

Fig. 6. (A): KEGG enrichment bubble of metabolites in the different treatments (control, L-NAME and NOR-3). (B): The connection plot of pathways related to energy metabolism development.

tion results of metabolite among three different groups (Zhang et al., 2018).

3.5.2. Orthogonal projections to latent structures discriminant analysis (OPLS-DA)

In order to find out the significantly different metabolites between L-NAME and NOR-3 groups, OPLS-DA model was established. The OPLS-DA model could distinguish the L-NAME and NOR-3 groups (Fig. 4B). A cross-validation analysis with 200 permutation tests showed that the intercepts of R^2 and Q^2 were 0.585 and − 0.429, respectively. The result indicates that the OPLS-DA model was reliable and statistically valid (Fig. 4C). Variable importance in projection (VIP) was calculated aiming to screen the significantly different metabolites between the two groups, and VIP value >1.0 was used as the screening criterion (Zhang, Zhang, & Xing, 2021). A total of 16 metabolites (glyceraldehyde 3-phosphate, dihydroxyacetone phosphate, adenosine diphosphate, adenosine diphosphate glucose, malate, acetyl-coa, cis-aconitate, oxaloacetate, glutamate, succinate, pyruvate, fumarate, citrate, cAMP, guanosine triphosphate and ATP) were finally discriminated as significantly different metabolites (Fig. 4D).

3.5.3. Hierarchical cluster analysis (HCA)

To visualize the relationship and the differences in expression patterns of metabolites in different groups, HCA heatmap was performed. As shown in **Fig. S3**, L-NAME group was separated from NOR-3 and control groups while NOR-3 group was separated from control group. These results indicate that the metabolite patterns were clearly changed after regulating the level of protein S-nitrosylation, which is also in concert with the PCA result.

3.6. Correlation analysis of metabolites

For further analyzing the correlation of different metabolites, correlation analysis was performed. The metabolites in the glycolysis pathway were closely related to the metabolites in the TCA cycle, indicating that different levels of protein S-nitrosylation could affect both the TCA cycle and glycolysis in the *in vitro* model (Fig. 5 **and Table S2**). Meanwhile, a significant positive correlation was also observed between the contents of lactate and pyruvate ($R = 0.713$; $p < 0.01$). However, the contents of pyruvate and G6P showed a significant negative correlation ($R = -0.603$; $p < 0.05$). For the TCA cycle, the reaction catalyzed by isocitrate dehydrogenase is the rate-limiting step in the TCA cycle. There was a negative correlation between the contents of pyruvate and isocitrate ($R = -0.501$; $p > 0.05$). Moreover, the contents of pyruvate and alpha-ketoglutarate showed a positive correlation ($R = 0.470$; $p > 0.05$). These results demonstrate that metabolites have a common metabolic pool and are in dynamic equilibrium with each other (Zhang et al., 2018).

3.7. Metabolic pathway analysis

Metabolic pathway analysis is an important method in the reconstruction of biochemical reaction networks (Sin et al., 2015). To investigate the effect of protein S-nitrosylation on energy metabolism, the metabolic pathways of differential metabolites among L-NAME, NOR-3 and control groups were carried out by using Kyoto Encyclopedia of Genes and Genomes (KEGG; https://www.kegg.jp/kegg/). Ten related metabolic pathways were visualized in Fig. 6 **(A)**. Based on KEGG data library, four metabolic pathways were identified including all significantly differential metabolites screened by OPLS-DA model. Four metabolic pathways (glycolysis, TCA cycle, purine metabolism and PPP) were connected and summarized. As shown in Fig. 6 **(B)**, G6P connected the PPP with glycolytic metabolism, pyruvate built a bridge between glycolytic metabolism and lactate biosynthesis, alpha-ketoglutarate was associated with glutamate metabolism and TCA cycle, and oxaloacetate was a relation link between glycolytic metabolism and TCA cycle.

Similarly, Welzenbach et al. (2016) also identified four same metabolic pathways and the change of these metabolic pathways was related to meat quality including pH and color. Glycolytic metabolism (contained 10 metabolites) and TCA cycle (contained 12 metabolites) were further screened out as the major energy metabolism pathways influenced by protein S-nitrosylation according to the number of differential metabolites in the metabolic pathways. Consistent with our results, Matarneh et al. (2021) also demonstrated that TCA cycle and glycolysis were important metabolic pathways in postmortem muscle. Hence, the present study indicates that glycolysis and TCA cycle were important metabolic pathways affected by different levels of protein S-nitrosylation to regulate the energy metabolism in the *in vitro* model.

4. Conclusion

Current study showed that NOR-3 treatment led to a greater level of protein S-nitrosylation. Sixteen significantly differential energy metabolites were identified by UPLC-MS/MS in three groups. These results demonstrated that metabolites had a common metabolic pool and were in dynamic equilibrium with each other. In addition, glycolysis and TCA cycle were significant metabolic pathways affected by different levels of protein S-nitrosylation to regulate the energy metabolism in the *in vitro* model. Thus NO can be involved in regulating the energy metabolism by the pathway of protein S-nitrosylation. Further study should be focused on the relationship between the function of mitochondria and protein S-nitrosylation.

CRediT authorship contribution statement

Wenwei Lu : Conceptualization, Data curation, Methodology, Software, Formal analysis, Visualization, Writing – original draft, Writing – review & editing, Investigation, Validation. **Qin Hou :** Writing – review & editing. **Jian Zhang :** Writing – review & editing. **Wangang Zhang :** Conceptualization, Supervision, Resources, Funding acquisition, Project administration.

Declaration of Competing Interest

The authors declare no competing financial interest.

Data availability

Data will be made available on request.

Acknowledgments

This work was financially supported by Agriculture Research System of China of MOF and MARA (CARS-35) and the earmarked fund for Jiangsu Agricultural Industry Technology System (JATS (2020) 425). We thank Shanghai Bioprofile Technology Company Ltd. for technological assistance in metabolomics experiment.

Appendix A. Supplementary data

Supplementary data to this article can be found online at https://doi.org/10.1016/j.meatsci.2022.109073.

References

Aliani, M., Farmer, L.J., Kennedy, J.T., Moss, B.W., & Gordon, A. (2013). *Post-slaughter changes in ATP metabolites, reducing and phosphorylated sugars in chicken meat. Meat Science, 94*(1), 55–62.

Bee, G., Anderson, A.L., Lonergan, S.M., & Huff-Lonergan, E. (2007). *Rate and extent of pH decline affect proteolysis of cytoskeletal proteins and water-holding capacity in pork. Meat Science, 76*(2), 359–365.

Bolaños, J.P., Delgado-Esteban, M., Herrero-Mendez, A., Fernandez-Fernandez, S., & Almeida, A. (2008). *Regulation of glycolysis and pentose–phosphate pathway by nitric oxide: Impact on neuronal survival. Biochimica et Biophysica Acta (BBA)-Bioenergetics*, *1777*(7–8), 789–793.

Brannan, R.G., & Decker, E.A. (2002). *Nitric oxide synthase activity in muscle foods. Meat Science*, *62*(2), 229–235.

Carafoli, E. (2002). *Calcium signaling: A tale for all seasons. Proceedings of the National Academy of Sciences*, *99*(3), 1115–1122.

Chouchani, E.T., Hurd, T.R., Nadtochiy, S.M., Brookes, P.S., Fearnley, I.M., Lilley, K.S., … Murphy, M.P. (2010). *Identification of S-nitrosated mitochondrial proteins by S-nitrosothiol difference in gel electrophoresis (SNO-DIGE): Implications for the regulation of mitochondrial function by reversible S-nitrosation. The Biochemical Journal*, *430*(1), 49–59.

Cônsolo, N.R.B., Rosa, A.F., Barbosa, L.C.G.S., Maclean, P.H., Higuera-Padilla, A., Colnago, L.A., & Titto, E.A.L. (2021). *Preliminary study on the characterization of longissimus lumborum dark cutting meat in Angus× Nellore crossbreed cattle using NMR-based metabolomics. Meat Science*, *172*, 108350.

Escames, G., López, L.C., Ortiz, F., López, A., García, J.A., Ros, E., & Acuña-Castroviejo, D. (2007). *Attenuation of cardiac mitochondrial dysfunction by melatonin in septic mice. The FEBS Journal*, *274*(8), 2135–2147.

Gao, W.W., Huang, M.Q., Chen, X., Chen, J.P., Zou, Z.W., Li, L.L., … Liu, Q.Z. (2021). *The role of S-nitrosylation of PFKM in regulation of glycolysis in ovarian cancer cells. Cell Death & Disease*, *12*(4), 1–14.

Hertz, L., & Chen, Y. (2017). *Integration between glycolysis and glutamate-glutamine cycle flux may explain preferential glycolytic increase during brain activation, requiring glutamate. Frontiers in Integrative Neuroscience*, *11*, 18.

Hou, Q., Liu, R., Tian, X.N., & Zhang, W.G. (2020). *Involvement of protein S-nitrosylation in regulating beef apoptosis during postmortem aging. Food Chemistry*, *326*, 126975.

Li, Y.P., Liu, R., Zhang, W.G., Fu, Q.Q., Liu, N., & Zhou, G.H. (2014). *Effect of nitric oxide on μ-calpain activation, protein proteolysis and protein oxidation of pork during postmortem aging. Journal of Agricultural and Food Chemistry*, *62*, 5972–5977.

Liu, R., Warner, R.D., Zhou, G.H., & Zhang, W.G. (2018). *Contribution of nitric oxide and protein S-nitrosylation to variation in fresh meat quality. Meat Science*, *144*, 135–148.

Liu, R., Zhang, C.Y., Xing, L.J., Zhang, L.L., Zhou, G.H., & Zhang, W.G. (2019). *A bioinformatics study on characteristics, metabolic pathways, and cellular functions of the identified S-nitrosylated proteins in postmortem pork muscle. Food Chemistry*, *274*, 407–414.

Matarneh, S.K., Beline, M., Silva, S.D.L., Shi, H., & Gerrard, D.E. (2018). *Mitochondrial F1-ATPase extends glycolysis and pH decline in an in vitro model. Meat Science*, *137*, 85–91.

Matarneh, S.K., Yen, C.N., Bodmer, J., El-Kadi, S.W., & Gerrard, D.E. (2021). *Mitochondria influence glycolytic and tricarboxylic acid cycle metabolism under postmortem simulating conditions. Meat Science*, *172*, 108316.

Merry, T.L., Steinberg, G.R., Lynch, G.S., & Mcconell, G.K. (2009). *Skeletal muscle glucose uptake during contraction is regulated by nitric oxide and ROS independently of AMPK. AJP Endocrinology and Metabolism*, *298*, 577–585.

Moutinho, A., Hussey, P.J., Trewavas, A.J., & Malho, R. (2001). *cAMP acts as a second messenger in pollen tube growth and reorientation. Proceedings of the National Academy of Sciences*, *98*(18), 10481–10486.

Muroya, S., Oe, M., Nakajima, I., Ojima, K., & Chikuni, K. (2014). *CE-TOF MS-based metabolomic profiling revealed characteristic metabolic pathways in postmortem porcine fast and slow type muscles. Meat Science*, *98*(4), 726–735.

Sin, Y.L., Li, C.T., Saberi, M., Deris, S., Subair, S., & Ibrahim, Z. (2015). *A review on metabolic pathway analysis in biological production. Mini-Reviews in Organic Chemistry*, *12*(6), 506–523.

Stamler, J.S., & Meissner, G. (2001). *Physiology of nitric oxide in skeletal muscle. Physiological Reviews*, *81*(1), 209–237.

Wang, Y.Y., Liu, R., Hou, Q., Tian, X.N., Fan, X.Q., Zhang, W.G., & Zhou, G.H. (2020). *Comparison of activity, expression and S-nitrosylation of glycolytic enzymes between pale, soft and exudative and red, firm and non-exudative pork during post-mortem aging. Food Chemistry*, *314*, 126203.

Wang, Y.Y., Liu, R., Tian, X.N., Fan, X.Q., Shi, Y.W., Zhang, W.G., … Zhou, G.H. (2019). *Comparison of activity, expression, and S-nitrosylation of calcium transfer proteins between pale, soft, and exudative and red, firm, and non-exudative pork during post-mortem aging. Journal of Agricultural and Food Chemistry*, *67*(11), 3242–3248.

Warner, R.D., Dunshea, F.R., Ponnampalam, E.N., & Cottrell, J.J. (2005). *Effects of nitric oxide and oxidation in vivo and postmortem on meat tenderness. Meat Science*, *71*(1), 205–217.

Warner, R.D., Kauffman, R.G., & Greaser, M.L. (1997). *Muscle protein changes post mortem in relation to pork quality traits. Meat Science*, *45*(3), 339–352.

Wells, G.D., Selvadurai, H., & Tein, I. (2009). *Bioenergetic provision of energy for muscular activity. Paediatric Respiratory Reviews*, *10*(3), 83–90.

Welzenbach, J., Neuhoff, C., Looft, C., Schellander, K., Tholen, E., & Große-Brinkhaus, C. (2016). *Different statistical approaches to investigate porcine muscle metabolome profiles to highlight new biomarkers for pork quality assessment. PLoS One*, *11*(2), e0149758.

Young, M.E., Radda, G.K., & Leighton, B. (1997). *Nitric oxide stimulates glucose transport and metabolism in rat skeletal muscle in vitro. The Biochemical Journal*, *322*(1), 223–228.

Yu, Q.Q., Tian, X.J., Shao, L.L., Li, X.M., & Dai, R.T. (2019). *Targeted metabolomics to reveal muscle-specific energy metabolism between bovine longissimus lumborum and psoas major during early postmortem periods. Meat Science*, *156*, 166–173.

Zhang, J., Ye, Y.F., Sun, Y.Y., Pan, D.D., Ou, C.R., Dang, Y.L., … Wang, D.Y. (2018). *1H NMR and multivariate data analysis of the differences of metabolites in five types of dry-cured hams. Food Research International*, *113*, 140–148.

Zhang, J., Zhang, W.G., & Xing, L.J. (2021). *Effects of ultrasound on the taste components from aqueous extract of unsmoked bacon. Food Chemistry*, *365*, 130411.

Zhang, L.L., Liu, R., Cheng, Y.P., Xing, L.J., Zhou, G.H., & Zhang, W.G. (2019). *Effects of protein S-nitrosylation on the glycogen metabolism in postmortem pork. Food Chemistry*, *272*, 613–618.

Zhang, W.G., Marwan, A., Samaraweera, H., Lee, E.J., & Ahn, D.U. (2013). *Breast meat quality of broiler chickens can be affected by managing the level of nitric oxide. Poultry Science*, *92*, 3044–3049.

Zhang, Z.W., Luo, S., Zhang, G.C., Feng, L.Y., Zheng, C., Zhou, Y.H., … He, Y.K. (2017). *Nitric oxide induces monosaccharide accumulation through enzyme S-nitrosylation. Plant, Cell & Environment*, *40*(9), 1834–1848.

Zhu, Q.N., Xing, L.J., Hou, Q., Liu, R., & Zhang, W.G. (2021). *Proteomics identification of differential S-nitrosylated proteins between the beef with intermediate and high ultimate pH using isobaric iodoTMT switch assay. Meat Science*, *172*, 108321.